Witten-Veneziano relation, quenched QCD, and overlap fermions

Thomas DeGrand

Department of Physics, University of Colorado, Boulder, Colorado 80309

Urs M. Heller

CSIT, Florida State University, Tallahassee, Florida 32306-4120

(MILC Collaboration)

The quarks in quenched QCD have an anomalous self-interaction in the flavor singlet Goldstone boson channel. This coupling is extracted from a graph with disconnected quark lines, and is used to infer the mass of the eta-prime meson in full QCD. When the fermions are described by an overlap action, the Witten-Veneziano relation is an exact relation between the topological susceptibility (as defined through fermionic zero modes) and the inferred value of the eta-prime mass. Using an overlap action we compute the hairpin amplitude and determine the fermion zero-mode susceptibility, the inferred eta-prime mass and other parameters characterizing the low energy chiral properties of quenched QCD.

I. INTRODUCTION

The physics of the flavor singlet pseudoscalar eta-prime meson has long been a source of puzzles.

(i) The eta-prime is not a Goldstone boson because of the presence of the axial anomaly.

(ii) The eta-prime propagator in full QCD involves a set of connected and disconnected quark-line diagrams. Summing a plausible subset of these diagrams (see Fig. 1) produces a shift in the eta-prime mass away from the masses of the true Goldstone bosons. But what gauge field dynamics "fills in the white space" between the quark loops?

(iii) In the limit of a large number of colors N_c, the eta-prime mass is expected to scale as $1/N_c$ as opposed to the masses of non-Goldstone mesons, which remain order 1. A mass formula relating the eta-prime mass to the topological susceptibility has been derived by Witten and Veneziano [1]:

$$m_{\eta'}^2 + m_\eta^2 - 2m_K^2 = \mu_0^2 = \frac{4N_f\chi_T}{f_\pi^2} \qquad (1)$$

where χ_T is the topological susceptibility of the pure gauge theory, N_f is the number of flavors, and the pion decay constant, defined through $\langle 0|\bar\psi\gamma_0\gamma_5\psi|\pi\rangle = m_\pi f_\pi$, has the experimental value of 132 MeV. The right-hand side is formally $O(1/N_c)$ because $f_\pi \simeq \sqrt{N_c}$. The suppression of fermion loops at large N_c is similar to the absence of fermion loops in the quenched approximation, and lattice calculations of the topological susceptibility in quenched QCD (using pure gauge observables) give numbers with good numerical agreement with Eq. (1), when evaluated with the physical masses of the particles. It seems strange that this large-N_c formula should be quantitatively correct, since the eta-prime mass is not particularly small compared to the masses of other non-Goldstone boson mesons. [It is worth remarking that the flavor-nonsinglet pseudoscalar sector is also the home of other large-mass quantities: one example is the scale

of chiral symmetry breaking: $m_\pi^2/(m_u+m_d) \simeq 3$ GeV. The physical eta-prime mass is less than one-third of that number.]

The relation of these statements to each other is an ongoing source of controversy. Lattice simulations can in principle contribute to the discussion and, indeed, there have been many studies of the eta-prime on the lattice, dating back to the earliest days of simulation (a partial list includes [2–8]). Most of these studies have been in the quenched approximation, where the mass of the eta-prime is inferred from the size of the hairpin graph compared to the connected graph and compared to the topological susceptibility. When the contribution of individual eigenmodes of the Dirac operator to the hairpin graph is computed, it is often seen that the low-lying eigenmodes make a substantial contribution to the hairpin graph.

This paper is another calculation of the hairpin diagram in quenched QCD. Why revisit this question yet again? The reason is that the calculations presented here are done with a fermion action which respects chiral symmetry on the lattice via the Ginsparg-Wilson relation [9]: an overlap [10] action. All previous studies of the eta-prime were done with lattice actions which have chiral symmetry breaking artifacts: for Wilson-type fermions, for example, real eigenmodes of the Dirac operator are not zero modes nor are they eigenstates of γ_5. Since the properties of the eta-prime are known to be intertwined with the anomaly, one would expect that calculations with exact lattice chiral symmetry might be more
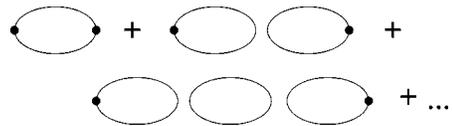
FIG. 1. A plausible set of quark line graphs, which sum into a geometric series to shift the eta-prime mass away from the mass of the flavor nonsinglet pseudoscalar mesons. In the quenched approximation, only the first two terms in the series survive as the "direct" and "hairpin" graphs.

revealing for the study of the eta-prime.

Indeed that is the case: when the fermions are described by an overlap action, the Witten-Veneziano (WV) relation is an exact relation between the expectation value of the hairpin diagram—which is given by the susceptibility of fermion zero modes—and the anomalous coupling between two flavor singlet Goldstone bosons. Interpreting that coupling as the eta-prime mass and equating the zero mode susceptibility to the topological susceptibility yields Eq. (1).

To see this, first recall some facts about the overlap action:

The eigenmodes of any massless overlap operator $D(0)$ are located on a circle in the complex plane of radius x_0 with a center at the point $(x_0, 0)$. The corresponding eigenfunctions are either chiral (for the eigenmodes with real eigenvalues located at $\lambda = 0$ or $\lambda = 2x_0$) or nonchiral and paired; the two eigenvalues of the nonchiral modes are complex conjugates. The massive overlap Dirac operator is conventionally defined to be

$$D(m_q) = \left(1 - \frac{m_q}{2x_0}\right)D(0) + m_q \qquad (2)$$

and it is also conventional to define the propagator so that the chiral modes at $\lambda = 2x_0$ are projected out:

$$\hat{D}^{-1}(m_q) = \frac{1}{1 - m_q/(2x_0)}\left(D^{-1}(m_q) - \frac{1}{2x_0}\right). \qquad (3)$$

For a summary of useful formulas, see Ref. [11] (for the special case $x_0 = 1/2$).

Now consider the hairpin diagram involving a single flavor of quarks, where the source and sink (black dots in Fig. 1) are the local pseudoscalar density, $\bar{\psi}\gamma_5\psi$. The hairpin diagram then is just

$$H(x,y) = \langle \text{Tr}\,\gamma_5 \hat{D}(x,x)^{-1}\,\text{Tr}\,\gamma_5 \hat{D}(y,y)^{-1}\rangle. \qquad (4)$$

Because only zero modes are chiral, the volume integral of the hairpin graph is proportional to the zero mode susceptibility [11]:

$$\frac{1}{V}\sum_{x,y} H(x,y) = \frac{\langle Q^2\rangle}{Vm_q^2} = \frac{\chi}{m_q^2}, \qquad (5)$$

where Q is just the number of zero modes, the difference of positive and negative chirality zero modes, $Q = n_+ - n_-$. Regardless of any dynamical model used to describe the hairpin graph, we expect to see a large contribution from zero modes to $H(x,y)$ itself, since only they contribute to the susceptibility.

In quenched QCD, as described by quenched chiral perturbation theory [12], there is an anomalous coupling of two Goldstone bosons in the flavor singlet channel, parametrized by a coupling with the dimensions of a squared mass. The hairpin graph is analyzed as if each of its quark loops is a propagator for an ordinary pseudoscalar Goldstone meson. That is, the momentum space amplitude for the connected graph is

$$C(q) = f_P \frac{1}{q^2 + m_\pi^2} f_P \qquad (6)$$

while the hairpin amplitude involving a single flavor is

$$H(q) = f_P \frac{1}{q^2 + m_\pi^2}\frac{\mu_0^2}{N_f}\frac{1}{q^2 + m_\pi^2}f_P. \qquad (7)$$

The quantity μ_0^2 is the squared mass of the "quenched approximation eta-prime" in the chiral limit. [The factor $1/N_f$ converts the single-flavor graph into the expectation of the eta-prime mass in N_f-flavor QCD, since each closed loop has a multiplicity of N_f, and the wave function (vertex) is scaled by a factor of $1/\sqrt{N_f}$.] In full QCD the correlator which gives the mass of the isosinglet meson is the difference $C(t) - N_f H_{full}(t)$, and $H(t)$ is supposed to represent the first term in a geometric series, which sums up to

$$C(q) - N_f H_{full}(q) = C(q) - N_f H(q) + \cdots$$

$$= f_P \frac{1}{q^2 + m_\pi^2 + \mu_0^2}f_P, \qquad (8)$$

shifting the squared mass of the meson from m_π^2 to $m_\pi^2 + \mu_0^2$. In these expressions, $f_P = \langle 0|\bar{\psi}\gamma_5\psi|\pi\rangle = m_\pi^2 f_\pi/(2m_q)$ from the PCAC (partial conservation of axial-vector current) relation. Computing the susceptibility directly from Eq. (7) gives

$$\frac{1}{V}\sum_{x,y} H(x,y) = \frac{f_P^2}{m_\pi^4}\frac{\mu_0^2}{N_f} = \frac{\mu_0^2 f_\pi^2}{4N_f m_q^2}. \qquad (9)$$

Equating Eqs. (5) and (9), we obtain the Witten-Veneziano relation $\mu_0^2 = 4N_f\chi/f_\pi^2$, where χ is the zero mode susceptibility.

This simple derivation of the Witten-Veneziano relation from the overlap action uses only the quenched approximation, without any reference to the large N_c limit. The crucial ingredient is the fact that the hairpin graph, in the quenched approximation, takes the form of Eq. (7). Conventional derivations of the Witten-Veneziano relation in unquenched QCD proceed rather differently: One begins by considering a correlator of the local topological charge density,

$$U(k) = \int d^4x\,\exp(ikx)\left\langle\left(\frac{g^2}{16\pi^2 N_c}F\tilde{F}(x)\right)\right.$$

$$\left.\times\left(\frac{g^2}{16\pi^2 N_c}F\tilde{F}(0)\right)\right\rangle \qquad (10)$$

which is assumed to be dominated by an eta-prime resonance plus other massive states:

$$U(k) = \frac{C_{\eta'}^2}{k^2 + m_{\eta'}^2} + \cdots \qquad (11)$$

with $C_{\eta'} = \langle 0|g^2/(16\pi^2 N_c)F\tilde{F}|\eta'\rangle$. Using the anomaly equation $2N_f[g^2/(16\pi^2 N_c)F\tilde{F}] = \partial_\mu J_5^\mu$ allows one to re-

place the gluonic matrix element by the matrix element of the divergence of the quark current. Computing the susceptibility by taking k to zero and setting the eta-prime and pion decay constants equal, so $\langle 0|\partial_\mu J_5^\mu|\eta'\rangle = \sqrt{N_f} m_{\eta'}^2 f_\pi$, gives the Witten-Veneziano relation. The difference is that here the eta-prime really is a propagating particle, whereas in the quenched approximation the mass is just the value of the two-boson coupling. Note also that in the derivation we have just given, the topological susceptibility is replaced by the squared fluctuation in the number of fermionic zero modes. The $k \to 0$ limit of $U(k)$ is a problematic one due to the contribution of contact terms [13].

A third kind of derivation of the Witten-Veneziano relation has recently been given by Giusti *et al.* [14]. Building on derivations of the Ward identity for the flavor singlet axial vector current by Hasenfratz, Laliena and Niedermayer [15] and Lüscher [16], they show that the Witten-Veneziano relation for overlap fermions involves the zero mode susceptibility, not the topological susceptibility. However, they assume that the axial current correlator is saturated by a propagating eta-prime resonance, keeping Eq. (11). That does not occur in quenched approximation, where the flavor singlet channel propagator is given by Eq. (7).

In full QCD the hairpin correlator is a single particle propagator, but the correlator which gives the eta-prime mass is given by $C(q) - N_f H_{full}(q)$. Here $H_{full}(q)$ still couples to zero modes, but in order for the difference to couple only to the eta prime, the hairpin must have a piece which cancels the connected correlator $C(q)$, the susceptibility of which is order $1/m_\pi^2$. Then $H_{full}(0) = 1/m_\pi^2 + \cdots = \chi/m_q^2$ and one finds [11,17] the expected result [18] that $\chi \simeq m_q$. The eta-prime mass is only connected to the zero-mode susceptibility through terms which are higher order in the quark mass.

We will compute the zero mode susceptibility both directly and via a calculation of the hairpin graph, and compare the results. In practice, in common with all lattice calculations of matrix elements, we will extract μ_0^2 from correlators using extended sources and sinks. We infer that the mass relation persists, regardless of the choice of source and sink, by assuming that the hairpin graph is a two-point vertex of pseudoscalar mesons, as required by quenched chiral perturbation theory.

We will see that Eq. (5) produces a measurement of μ_0^2 and χ with a somewhat larger statistical uncertainty than one would get from a direct measurement (counting zero modes) of $\langle Q^2 \rangle$. This happens despite the fact that in the fit to the hairpin, one is using information from many points of the lattice, while counting zero modes gives just one number per lattice. The signal from the many points just shows very strong correlations from point to point, and the actual hairpin graph is computed at nonzero quark mass and must be extrapolated to the chiral limit.

II. LATTICE CALCULATION

The overlap action used in these studies [19] is built from an action with nearest- and next-nearest-neighbor couplings, and APE-blocked links [20]. Eigenmodes of the massless overlap Dirac operator $D(0)$ are constructed from eigen-

modes of the Hermitian Dirac operator $H(0) = \gamma_5 D(0)$, using an adaptation of a conjugate gradient algorithm of Bunk *et al.* and Kalkreuter and Simma [21]. These eigenmodes are used to precondition the calculation of the quark propagator and to construct quark propagators truncated to some number of low-lying eigenmodes.

The data set is generated in the quenched approximation using the Wilson gauge action at a coupling $\beta = 5.9$. The nominal lattice spacing is $a = 0.13$ fm from the measured rho mass (a value we prefer; see below) or inferred to be 0.11 fm from the Sommer parameter using the interpolation formula of Ref. [22]. We worked with lattices with $12^3 \times 24$ sites. Quark masses in lattice units are $am_q = 0.02$, 0.04, and 0.06, corresponding to pseudoscalar-to-vector meson mass ratios of $m_{PS}/m_V \simeq 0.5$, 0.61 and 0.67. The fermions have periodic boundary conditions in the spatial directions and anti-periodic temporal boundary conditions. We calculated the 20 smallest eigenvalue modes of $H^2(0)$ in the chiral sector of the minimum eigenvalue, and reconstructed the degenerate opposite chirality eigenstate of $H^2(0)$ for each nonzero eigenvalue mode. These modes are then recoupled into eigenmodes of $D(0)$. Their eigenvalues have imaginary parts ranging up to $0.3/a - 0.35/a$, or about 500 MeV [23].

All correlators we measured will include a smearing function which averages the source of the propagator over a localized spatial volume, in order that the meson source resemble an actual hadron wave function. The hairpin correlator that we measure is

$$H_\Gamma(t) = \frac{1}{T} \sum_{t_1} \left\langle \sum_x \sum_y \mathrm{Tr}\, L_\Gamma(x, t+t_1)\,\mathrm{Tr}\, L_\Gamma(y, t_1) \right\rangle \tag{12}$$

where the single fermion loop is

$$L_\Gamma(x,t) = \sum_{x_1, x_2} \Phi(x_1 - x)\Phi(x_2 - x)\langle \bar\psi(x_1,t)\Gamma\psi(x_2,t)\rangle. \tag{13}$$

Γ is a product of Dirac matrices: γ_5 and $\gamma_0\gamma_5$ are studied for the eta prime.

The connected correlator uses the same (separable) weighting function

$$C_\Gamma(t) = \left\langle \sum_x \sum_{x_1, x_2} \Phi(x_1 - x)\Phi(x_2 - x)\bar\psi(x_1,t)\Gamma\psi(x_2,t) \right.$$

$$\left. \times \sum_{y_1, y_2} \Phi(y_1)\Phi(y_2)\bar\psi(y_1,0)\Gamma\psi(y_2,0) \right\rangle. \tag{14}$$

We take the weighting function to be a Gaussian, $\Phi(x) = \exp(-|x|^2/r_0^2)$, of width $r_0 = 3a$.

In coordinate space we fit

$$C(t) = \frac{Z}{2m}\{\exp(-mt) + \exp[-m(T-t)]\} \tag{15}$$

and, since

$$H(q) = -\frac{\mu_0^2}{N_f}\frac{\partial}{\partial m^2}C(q), \tag{16}$$

the coordinate space hairpin is

$$H(t) = \frac{Z}{4m^3}\frac{\mu_0^2}{N_f}\{(1+mt)\exp(-mt)$$

$$+[1+m(T-t)]\exp[-m(T-t)]\}. \tag{17}$$

We break up the computation of the single loop into two terms. The first term includes the contribution of the low eigenmodes of D, and is done exactly (for those modes): Chiral eigenmodes of $D(0)^\dagger D(0)$ are labeled as $\phi_{j\pm}(x,t)$, the plus or minus sign corresponding to the chirality. They have associated eigenvalues λ_j. These modes are recoupled into eigenmodes of $\hat{D}^{-1}(m)$. The only mode mixing occurs between degenerate eigenmodes of $D(0)^\dagger D(0)$. The single fermion loop becomes

$$L_1(x,t) = \sum_j^N [\mathrm{Tr}\,\alpha_{j+}\Psi_{j+}^\dagger(x,t)\Gamma\Psi_{j+}(x,t)$$

$$+\mathrm{Tr}\,\alpha_{j-}\Psi_{j-}^\dagger(x,t)\Gamma\Psi_{j-}(x,t)], \tag{18}$$

where $\Psi_{j\pm}(x,t) = \Sigma_{x_1}\Phi(x-x_1)\phi_{j\pm}(x_1,t)$ is the convolution of the jth eigenmode with the smearing function Φ. Here, defining $\mu = m/(2x_0)$, $\epsilon_j = \lambda_j/(2x_0)$, the $\alpha_{j\pm}$, the eigenvalues of $\hat{D}^{-1}(m)$, are

$$\alpha_{j\pm} = \frac{1}{2x_0}\frac{\mu(1-\epsilon_j^2)\pm i\epsilon_j\sqrt{1-\epsilon_j^2}}{\epsilon_j^2+\mu^2(1-\epsilon_j^2)}. \tag{19}$$

For zero modes only one term in the brackets in Eq. (18) exists.

The second part of the loop is computed using a stochastic estimator. We cast a vector of Gaussian random numbers $|r(x,t)\rangle$ on every site of the lattice, projected the modes used in L_1 from it (so $|r_1\rangle = |r\rangle - \Sigma_j|j\rangle\langle j|r\rangle$), convoluted $|r_1\rangle$ with the smearing function, and used this vector as the source for a propagator. A final convolution of the propagator with the source vector produced a noisy estimator for the difference $L(x,t) - L_1(x,t)$. We averaged over 12 random sources per lattice. Each source was broken into two opposite chirality pieces, so a total of 24 inversions, restricted to a single chirality sector each, were done per configuration.

In retrospect, our simple stochastic estimator did not produce a useful signal. We first generated a 40-lattice data set, on which we found the complete hairpin correlator, from both low modes and the stochastic estimator of high modes. For the pseudoscalar hairpin, all of the signal is contained in the low eigenmodes, which we captured exactly. Even so, we did not have a good enough signal from 40 lattices to analyze the hairpin graph, so we generated an additional 40 lattices. On these lattices we did an ordinary spectroscopy calculation for the connected diagram and computed the hairpin from the low modes. For our version of the overlap, the cost of finding the eigenmodes in addition to constructing ordinary propaga-
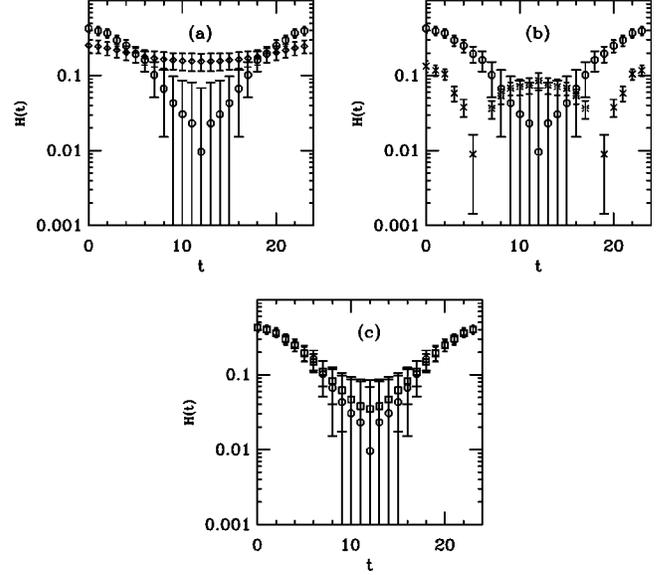
FIG. 2. Contribution to the pseudoscalar hairpin for the $am_q = 0.04$ data set from various subsets of eigenmodes: In all figures the full propagator is shown by octagons. In panel (a), the zero mode contribution is given by diamonds. In (b) the contribution of all nonzero modes is shown by crosses (where the contribution is positive) and bursts (where it is negative). In (c) the contribution of the lowest 20 modes of $D^\dagger D$ is shown by squares.

tors is negligible because the eigenmodes can be used to precondition the conjugate gradient calculation of propagators. At 24 inversions per lattice, a stochastic evaluation of the higher mode contribution is about twice as costly as an ordinary propagator calculation.

We did not experiment with more sophisticated noise reduction methods [24].

III. RESULTS

It is an interesting exercise to ask how the contributions of different sets of eigenmodes contribute to the pseudoscalar hairpin correlator. We find that the low modes completely saturate the hairpin graph at all mass values studied. Because the plots are rather cluttered, we show results for only one mass value, $am_q = 0.04$, in Fig. 2: The full correlator, including the low modes treated exactly and the high modes computed using the noisy estimator, is shown by octagons. Completely overlapping these points is the correlator built of the lowest 20 eigenmodes of $D^\dagger D$.

The zero mode piece is shown by diamonds. At large quark mass there is a rather strong interference between the zero mode contribution and the nonzero modes, which pulls the full propagator down. Since the low modes themselves saturate the correlator, this interference must be dominated by them.

Finally, the contribution of the nonzero modes by themselves is positive at short distance but becomes negative above a separation of $t \geq 7$ lattice spacings. We have displayed this by changing the plotting symbol for this contribution from crosses, when the signal is positive, to bursts, where it becomes negative.
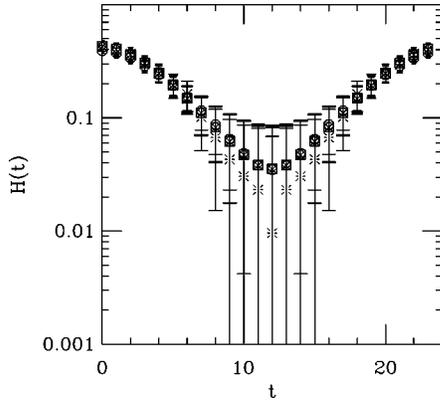
FIG. 3. Saturation of the pseudoscalar hairpin graph at am_q $=0.04$ by 5, 10, 15, and 20 eigenmodes of $H(0)^2$ (with symbols octagons, diamonds, squares, and crosses). Bursts show the full correlator.

It is easy to understand why nonzero modes contribute negatively at large separation. The jth pair of nonchiral modes contribute a term to the hairpin of

$$\hat{H}(t) = \frac{1}{T} \sum_{t'} \sum_{j,j'} \sum_{x,x'} \alpha_j \alpha_{j'} \langle \Omega_j(x,t+t')\Omega_{j'}(x',t') \rangle \tag{20}$$

where [see Eq. (18)]

$$\Omega_j(x,t) = \sum_{x_1,x_2} \Phi(x_1-x)\Phi(x_2-x)$$
$$\times \phi_j(x_1,t)^{\dagger}\gamma_5\phi_j(x_2,t) \tag{21}$$

is a local smearing of the chiral density of the jth mode. The nonzero modes have zero overall chirality and so at large distance the correlation function of the chiral density must become negative. This can be seen even on a single configuration. This behavior has been observed in the eigenmode studies of Ref. [23]. It may be more than a coincidence that these authors saw the chirality autocorrelator (for the same data set as we studied here) becoming negative around a distance of 6 or 7 lattice spacings.

Could we have used fewer modes? Figure 3 shows the contributions to the hairpin correlator of the lowest 5, 10, 15, and 20 modes of $H(0)^2$, for the $am_q=0.04$ data set. The pictures for the other masses are virtually identical. We could have kept only five modes of $H(0)^2$ and almost completely saturated the hairpin correlator, in our particular simulation volume.

We have performed correlated fits to the connected and hairpin pseudoscalar graphs to Eqs. (15) and (17) and extracted lattice predictions for μ_0^2/N_f. An example of a fit, to the $am_q=0.04$ low-eigenmode hairpin, is shown in Fig. 4. The error bars on the points are the naive ones and do not show the considerable correlation between the data from different time slices. A set of fits, for a time slice range of $t_{min}=3$ out to $t_{max}=12$, is shown in Fig. 5. We have separated fits to using hairpin correlators with truncated quark propagators and fits using the full quark propagator in the
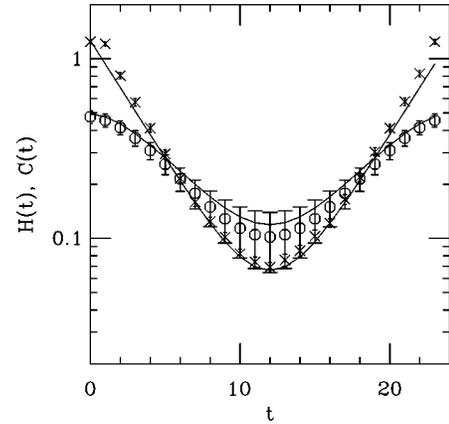
FIG. 4. Connected correlator (crosses) and hairpin (octagons), for the lowest 20 eigenmode hairpin, at bare quark mass am_q $=0.04$, showing the result of a correlated fit to the two correlators over the range $t=6-18$ (folded to $6-12$).

hairpin. All of the fits to the low-mode hairpin have good confidence levels for $t_{min} \gtrsim 5-6$. Pion masses are also a byproduct of the fit. Their values are stable for $t_{min} \gtrsim 3-4$ and equal within uncertainties to the results of fits to pion propagators in isolation.

The "full" signal is much noisier than the low mode truncation (even more than one would expect, knowing that the low mode data set is twice as big), and since both are equal within uncertainties, we quote the latter. Our chosen best fits, typically over a range $6-12$, are shown in Table I and plotted in Fig. 6. We have also extrapolated our results for μ_0^2/N_f to zero quark mass, assuming that μ_0^2/N_f is a linear function of the quark mass, using a single elimination jackknife.

Taking the lattice spacing from the rho mass, i.e., a $=0.13$ fm, and setting $N_f=3$ we predict μ_0 $=770(54)$ MeV$\times(a^{-1}/1520$ MeV$)$. Had we used the Sommer parameter to set the scale, i.e. $a=0.11$ fm or a^{-1} $=1770$ MeV, the mass would have come out about 16%
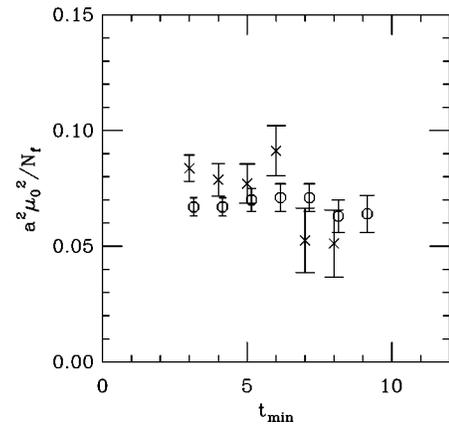
FIG. 5. Extracted pseudoscalar hairpin coupling μ_0^2/N_f from fits from distance t to 12 at $am_q=0.04$. Octagons show the results of fits to the hairpin correlator when the quark propagator is truncated to the lowest 20 eigenmodes (80 lattice data set) of $D^{\dagger}D$, and crosses show fits using the full propagators (40 lattice data set) in the hairpins.

TABLE I. Table of best-fit lattice parameters $a^2\mu_0^2/N_f$, af_π, $a^4\chi$, and δ as a function of quark mass and after jackknife extrapolations to zero mass.

m_0	$a^2\mu_0^2/N_f$	af_π	$a^4\chi$	δ
0.06	0.064(5)	0.102(2)	$1.67(21)\times10^{-4}$	0.077(8)
0.04	0.071(6)	0.104(4)	$1.95(34)\times10^{-4}$	0.083(17)
0.02	0.077(7)	0.106(7)	$2.24(40)\times10^{-4}$	0.088(20)
0	0.086(12)	0.108(14)	$2.52(58)\times10^{-4}$	0.093(28)

FIG. 7. Contribution to the $am_q=0.04$ $\gamma_0\gamma_5$ hairpin from low modes of $D^\dagger D$: 5 modes (small diamond with cross when positive, plus sign when negative), 10 modes (diamond and fancy cross), 15 modes (square and burst) and 20 modes (octagon and cross).

higher. This difference is, of course, a reflection of the inherent scale uncertainty in quenched QCD. Evaluating the left-hand side of Eq. (1) with observed particle masses gives $\mu_0=860$ MeV.

If the ''standard picture'' of the hairpin graph makes sense, we should be able to measure μ_0^2 using any interpolating field at the source and sink points. In particular, the axial vector ($\gamma_0\gamma_5-\gamma_0\gamma_5$) hairpin correlator is an interesting operator to study. No zero modes contribute to its hairpin correlator, and yet the pseudoscalar and axial vector hairpins should both give the same result for μ_0^2—the only difference in the two channels is that the coupling of the external current source to the pseudoscalar channel is different.

We attempted to measure μ_0^2 from this correlator, without success. We raise the point as a potentially interesting exercise if future high-statistics data become available.

At short distances this correlator is negative. At larger distances it swings positive, before disappearing into noise at large separation. (See Fig. 7 for the $am_q=0.04$ data set.) The node in the correlator makes it impossible to fit the data to the simple form of the hairpin we have used above. Notice from Fig. 7 that the hairpin correlator saturates more slowly with number of eigenmodes than the pseudoscalar correlator does: this, plus the nodes in the signal, makes the analysis impossible to do.

Now we return to the pseudoscalar correlator. To make contact with other chiral observables we need a lattice determination of f_π. We do this by measuring the pseudoscalar density P (as one vertex of a two-point function) and extract-

ing f_π from $m_\pi^2 f_\pi=2m_q\langle0|P|\pi\rangle$. Because the overlap action is chiral, the renormalization factors for the quark mass and the pseudoscalar density cancel. The pseudoscalar density is taken to be the naive operator $P(x)=\bar\psi\gamma_5\psi$. Note that because we use the ''subtracted'' propagator $\hat D^{-1}$, Eq. (3), our measurement is equivalent to the use of the ''order a^2 improved current'' $\bar\psi[1+D/(2x_0)]\gamma_5[1+D/(2x_0)]\psi$. The results of this exercise are shown in Fig. 8 and also given in Table I. Using again the lattice spacing from the rho mass we find in the chiral limit, obtained by linear extrapolation in the quark mass, $f_\pi=163(21)$ MeV. Had we used the Sommer parameter to set the scale we would have obtained $f_\pi=193(25)$ MeV. The latter number is obviously much larger than the experimental value of 132 MeV. We prefer the lattice spacing from the rho mass for phenomenology with the overlap fermions. A comparison of the point-to-point correlator in the pseudoscalar channel with instanton liquid model predictions also requires a large lattice spacing [25] of 0.13 fm. This correlator is proportional to $\langle0|P|\pi\rangle^2$.

The two parameters which are related to μ_0^2 are the zero mode susceptibility $\chi=\mu_0^2 f_\pi^2/(4N_f)$ and the parameter

FIG. 6. Pseudoscalar hairpin coupling μ_0^2/N_f in lattice units as a function of quark mass. The jackknife-extrapolated zero-quark-mass value is shown as the burst.
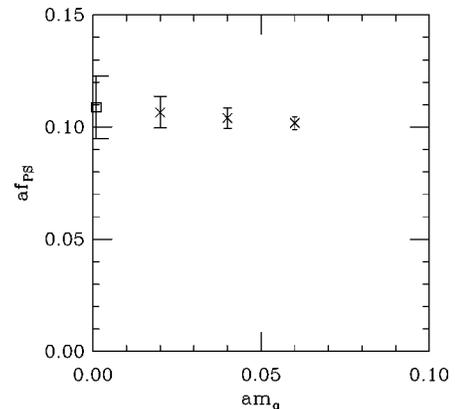
FIG. 8. Pseudoscalar decay constant (in lattice units) from this overlap action. Crosses are our data and a jackknife linear extrapolation to $m_q=0$ is shown by the square.
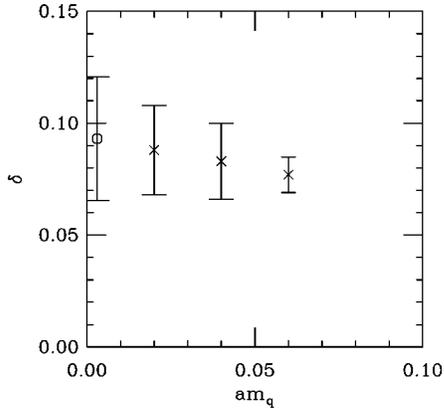
FIG. 9. The quenched chiral perturbation theory parameter δ $= \mu_0^2/(8\pi^2 N_f f_\pi^2)$ evaluated for $N_f = 3$. Crosses are our data and the extrapolated value at $m_q = 0$ is shown by the octagon.

which characterizes the strength of the hairpin contribution in quenched chiral perturbation theory [12], δ $= \mu_0^2/(8\pi^2 N_f f_\pi^2)$. We compute each of these parameters for each value of quark mass using a combination of single-elimination jackknife with correlated fits to pairs of two-point functions, and extrapolate the results linearly in the quark mass to $m_q = 0$. The resulting values are shown in Table I and in Figs. 9 and 10.

We can also perform a direct measurement of the topological susceptibility by counting zero modes: the topological charge Q on each configuration is just defined as the difference in number of opposite chirality zero modes in the configuration. For our 80 lattices, we find $\langle Q \rangle = 0.31 \pm 0.32$. We can (formally) eliminate the $\langle Q \rangle^2$ term from the average by combining our data with a parity-reversed copy of every lattice. (This is equivalent to the usual replacement of a propagator by its real part in conventional spectroscopy or matrix element calculations.) The zero modes give us the result $\langle Q^2 \rangle = 8.24 \pm 1.11$ and
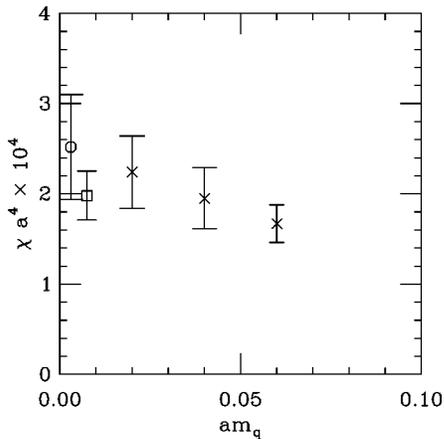
FIG. 10. The inferred zero mode susceptibility in lattice units from the hairpin graph $\chi = \mu_0^2 f_\pi^2/(4N_f)$ evaluated for $N_f = 3$. Crosses are our data and the extrapolated value at $m_q = 0$ is shown by the octagon. The susceptibility measured directly from zero modes is shown with the square.

$$a^4 \chi = \frac{\langle Q^2 \rangle}{V} = 1.98(27) \times 10^{-4}. \qquad (22)$$

This result agrees with the calculation of χ from μ_0^2. The quality of our signal is similar to what is seen in calculations of χ using pure gauge observables (lattice analogue of the topological charge density) with similar statistics. Converting this lattice number to a continuum result using the Sommer scale, as is conventional for the topological susceptibility, and taking the fourth root yields $\chi^{1/4} = 213(7)$ MeV from the direct counting of zero modes and $\chi^{1/4} = 226(12)$ MeV from the hairpin fit. Pure gauge studies produce similar numbers to what we see [26].

Obviously, with the scale set by the rho mass, the result would be about 16% lower, 180(6) and 191(11) MeV.

Our measurement of $\delta \simeq 0.093$ is a bit higher than recent determinations made using nonchiral actions [8,27,28], which measure $\delta \simeq 0.065$ [but somewhat smaller than what one would infer from the WV relation with physical masses, Eq. (1)]. The first calculation is done using clover fermions at $\beta = 5.7$. Clover fermions have real eigenmodes which make a nonvanishing contribution to Tr $\gamma_5 D^{-1}$. The overlap action counts each zero mode with unit weight. It is our experience that as the value of the real eigenvalue of a clover mode moves away from zero, the associated chirality also decreases, and so it is not surprising that our result is larger. The other two calculations determine δ from the small quark mass behavior of the pion mass, i.e. from observing quenched chiral logarithms, and can easily have quite different systematic uncertainties than our measurement.

We do not see any effects of quenched chiral logarithms in any observables. A fit to the pion mass in various channels (pseudoscalar, axial vector, difference of pseudoscalar and scalar) to the form suggested in Ref. [27], $m_\pi^2 = Cm_q[1 - \delta \log(Cm_q/\Lambda^2)]$, chooses δ's in the range 0.0–0.2, but with uncertainties from any fit also of the same order. The main effect of quenching we have seen is the presence of zero modes in the pseudoscalar and scalar channels; in contrast to the hairpin case, these are finite volume artifacts.

We do not have any useful signals from other channels. The scalar channel is dominated by zero and low eigenmodes, but the major structure in the channel is just the constant chiral condensate. In the vector channel the low-eigenmode correlator even has the wrong sign—it is negative over most of its range (compare Fig. 11). The absence of a signal could be consistent with a naive expectation from Zweig's rule, namely that the size of the hairpin in the vector channel is small. The low eigenmodes which we include exactly do not seem to make much of a contribution to disconnected diagrams in the vector channel, either. This feature is expected in instanton liquid models [29].

We would feel much more comfortable making these statements if we had a real signal [30].

IV. CONCLUSIONS

For overlap actions and in the quenched approximation, the Witten-Veneziano formula is an exact relation between the eta-prime mass inferred from the hairpin graph and the
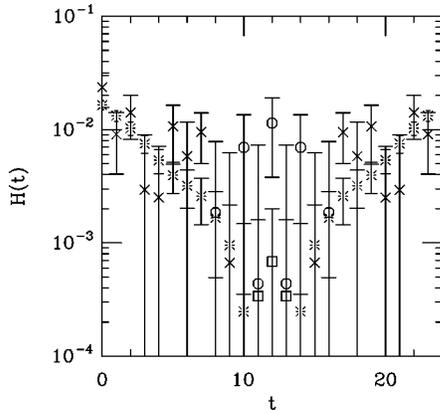
FIG. 11. Contribution to the $am_q = 0.04\gamma_i$ hairpin from the lowest 20 modes (square when positive, burst when negative) as compared to the full correlator (octagon when positive, cross when negative).

fermionic zero-mode susceptibility. However, the physics of the Witten-Veneziano relation in the overlap is rather different than in ''standard derivations'': the eta-prime is not a real particle; the mass we measure is the size of a quenched-artifact coupling between two flavor-singlet Goldstone bosons. For quenched QCD, the gauge configurations which ''fill in the white space'' in the hairpin diagram are the ones which produce zero modes. We have not addressed the question of what choice of contact term is needed to equate a particular definition of the topological susceptibility to the zero mode susceptibility.

The numbers we have found for the inferred eta-prime mass and the zero mode susceptibility are not all that different from previous results using nonchiral fermion actions. We believe that the theoretical underpinning of our calculation done with a chiral action is more reliable than any calculation done with a nonchiral action. We are well aware that our calculation is performed at only one value of the lattice spacing and that simulations at several lattice spacings are necessary for an honest extrapolation to a continuum value.

The strong coupling of low eigenmodes to the hairpin amplitude allowed us to perform the numerical simulation. This connection between the zero mode susceptibility and the coupling strength is not automatic for a nonchiral fermion action. Nevertheless, we expect that small eigenmodes of the Dirac operator will make a large contribution to the pseudoscalar hairpin correlator. We suggest that future studies of the hairpin graph, even done using nonchiral actions, can reduce the measurement noise by first finding all the zero or near-zero eigenmodes of the Dirac operator so that their contribution can be included exactly [31].

ACKNOWLEDGMENTS

[1] E. Witten, Nucl. Phys. **B156**, 269 (1979); G. Veneziano, *ibid.* **B159**, 213 (1979).

[2] H.W. Hamber, E. Marinari, G. Parisi, and C. Rebbi, Nucl. Phys. **B225**, 475 (1983).

[3] M. Fukugita, T. Kaneko, and A. Ukawa, Phys. Lett. **145B**, 93 (1984).

[4] S. Itoh, Y. Iwasaki, and T. Yoshie, Phys. Rev. D **36**, 527 (1987).

[5] Y. Kuramashi, M. Fukugita, H. Mino, M. Okawa, and A. Ukawa, Phys. Rev. Lett. **72**, 3448 (1994).

[6] M. Fukugita, Y. Kuramashi, M. Okawa, and A. Ukawa, Phys. Rev. D **51**, 3952 (1995).

[7] G. Kilcup, J. Grandy, and L. Venkataraman, Nucl. Phys. B (Proc. Suppl.) **47**, 358 (1996); L. Venkataraman, G. Kilcup, and J. Grandy, *ibid.* **53**, 259 (1997); L. Venkataraman and G. Kilcup, hep-lat/9711006.

[8] W. Bardeen, A. Duncan, E. Eichten, and H. Thacker, Phys. Rev. D **62**, 114505 (2000).

[9] P.H. Ginsparg and K.G. Wilson, Phys. Rev. D **25**, 2649 (1982).

[10] H. Neuberger, Phys. Lett. B **417**, 141 (1998); Phys. Rev. Lett. **81**, 4060 (1998).

[11] R.G. Edwards, U.M. Heller, and R. Narayanan, Phys. Rev. D **59**, 094510 (1999).

[12] Cf.S.R. Sharpe, Phys. Rev. D **46**, 3146 (1992); C.W. Bernard and M.F. Golterman, *ibid.* **46**, 853 (1992); C. Bernard, M. Golterman, J. Labrenz, S. Sharpe, and A. Ukawa, Nucl. Phys. B (Proc. Suppl.) **34**, 334 (1994); C.W. Bernard and M.F. Gol-

terman, Phys. Rev. D **53**, 476 (1996).

[13] For an old discussion of this problem, see R.J. Crewther, Riv. Nuovo Cimento **28**, 63 (1979); see also E. Seiler, Phys. Lett. B **525**, 355 (2002).

[14] L. Giusti, G.C. Rossi, M. Testa, and G. Veneziano, Nucl. Phys. **B628**, 234 (2002).

[15] P. Hasenfratz, V. Laliena, and F. Niedermayer, Phys. Lett. B **427**, 125 (1998).

[16] M. Lüscher, Phys. Lett. B **428**, 342 (1998).

[17] S. Chandrasekharan, Phys. Rev. D **60**, 074503 (1999).

[18] H. Leutwyler and A. Smilga, Phys. Rev. D **46**, 5607 (1992).

[19] MILC Collaboration, T. DeGrand, Phys. Rev. D **63**, 034503 (2001).

[20] APE Collaboration, M. Albanese *et al.*, Phys. Lett. B **192**, 163 (1987); M. Falcioni, M.L. Paciello, G. Parisi, and B. Taglienti, Nucl. Phys. **B251,** 624 (1985).

[21] See B. Bunk, K. Jansen, M. Lüscher, and H. Simma, DESY report, 1994; T. Kalkreuter and H. Simma, Comput. Phys. Commun. **93**, 33 (1996).

[22] ALPHA Collaboration, M. Guagnelli, R. Sommer, and H. Wittig, Nucl. Phys. **B535**, 389 (1998).

[23] T. DeGrand and A. Hasenfratz, Phys. Rev. D **64**, 034512 (2001).

[24] For examples of noise reduction in calculations of disconnected diagrams, see W. Wilcox, hep-lat/9911013; UKQCD Collaboration, C. McNeile and C. Michael, Phys. Rev. D **63**, 114503 (2001); SESAM Collaboration, T. Struckmann *et al.*,

ibid. **63**, 074503 (2001); J. Viehoff, Wupperthal thesis, 1999, Report No. DESY-THESIS-1999-036.

[25] T. DeGrand, Phys. Rev. D **64**, 094508 (2001).

[26] Cf.M. Teper, Nucl. Phys. B (Proc. Suppl.) **83**, 146 (2000).

[27] C.W. Bernard *et al.*, Phys. Rev. D **64**, 054506 (2001).

[28] CP-PACS Collaboration, S. Aoki *et al.*, Phys. Rev. Lett. **84**, 238 (2000).

[29] Cf.T. Schafer and E.V. Shuryak, Rev. Mod. Phys. **70**, 323 (1998).

[30] Cf.N. Isgur and H.B. Thacker, Phys. Rev. D **64**, 094507 (2001).

[31] K. Schilling, H. Neff, N. Eicker, T. Lippert, and J.W. Negele, Nucl. Phys. B (Proc. Suppl.) **106**, 227 (2002); **109**, 15 (2002).